Optimizing Forward Error Correction Codes for COFDM With Reduced PAPR

Francisco Sandoval, Gwenael Poitau, and François Gagnon

***Abstract*— Coded orthogonal frequency-division multiplexing (COFDM) is a popular modulation technique for wireless communication that guarantees reliable transmission of data over noisy wireless channels. However, a major disadvantage in implementing it is its resulting high peak to average power ratio (PAPR). Including forward error correction (FEC) in the orthogonal frequency division multiplexing (OFDM) system enables the avoidance of transmission errors. Nevertheless, the selected code may impact the value of PAPR. The objective of this paper is to analyze the impact of FEC on the PAPR for the COFDM system based on the autocorrelation of the signal, before the inverse fast Fourier transform (IFFT) block in the COFDM system, the evaluation of the complementary cumulative distribution function (CCDF) of PAPR, and the bit error rate (BER). The autocorrelation of the COFDM system is calculated based on a Markov chain model. From the results, we can reach a conclusion on the characteristics we need to consider in order to choose the codes relating to the PAPR performance in the COFDM system.**

***Index Terms*— Autocorrelation, coded OFDM, complementary cumulative distribution function, peak to average power ratio.**

I. Introduction

ORTHOGONAL frequency division multiplexing (OFDM) offers high spectrum efficiency and capacity, is flexible [1], and is a popular modulation technique for wireless digital communication systems such as 4G wireless communication systems, public safety systems, tactical communication systems, etc. Examples of such systems include IEEE 802.11 a/g/n/ac wireless LANs, Digital Audio Broadcasting (DAB), and Digital Video Broadcasting-Terrestrial (DVB-T).

The main implementation drawback of OFDM, however, is the high peak to average power ratio (PAPR) it produces [2]. When a significant PAPR appears in the transmitter, we require a power amplifier with wide dynamic range that is not power-efficient, and is expensive [3]. Therefore, many techniques have been proposed in the literature to reduce the PAPR [4], including selected mapping (SLM), partial transmit sequence (PTS), signal clipping and filtering.

Interestingly, in the literature, coding techniques such as block codes, Golay complementary sequences, and second-order Reed-Muller codes [3] are also used to reduce the PAPR. This suggests a possibility of using coding techniques to obtain both benefits, error control and PAPR reduction.

For example, Wilkinson and Jones [5] proposed PAPR reduction using a simple odd parity code (SOPC) which is based on a four-carrier signal with a 3/4 rate block code demonstrated that the PAPR could be reduced from 6.02 dB to 2.48 dB in the case of 4 bits, 3 bits could be used for data transmission and one for the odd parity check. Wilkinson and Jones [5] and Tao *et al.* [6] proposed the use of Golay complementary sequences to achieve the reduction of PAPR because the power spectrum of the Golay complementary sequences is approximately flat [7]. Another technique suggested for PAPR reduction is the complement block coding (CBC) [8]. The CBC is a code with detection and correction capabilities. The CBC can contribute in the reduction of the PAPR in the OFDM signal because it does not generate all-equal bit sequences. In the case of large frame size, the sub-block complementary coding (SBCC) [9] can be used. In SBCC, the information sequence is broken into several equal-sized sub-blocks, and each sub-block is encoded with a complementary error correction code.

This paper analyzes the impact of FEC on the PAPR for the COFDM system. As will be shown later, several of the FEC, frequently used in the current communication systems, caused degradation of the PAPR compared to the OFDM system. To that end, we conducted an analysis comparing the CCDF of PAPR to the autocorrelation of the COFDM signal before the inverse fast Fourier transform (IFFT) block. This allowed us to deduce the principal coding characteristics that generate the peak factor after the IFFT block, following which we could then choose the parameters of the coded structure in order to reduce the peak power. The analysis for convolutional codes of this study is emphasized; as well as a simple example of the linear block codes which is studied, based on the repetition codes.

Convolutional codes are widely used in current communication systems, for example, these are present in the audiovisual systems that require error correction in real time such as

Manuscript received May 29, 2018; revised November 12, 2018 and February 12, 2019; accepted April 5, 2019. Date of publication April 24, 2019; date of current version July 13, 2019. This work was supported in part by the Natural Sciences and Engineering Research Council of Canada and in part by Ultra Electronics TCS through the Industrial Research Chair in High Performance Wireless Emergency and Tactical Communications. The associate editor coordinating the review of this paper and approving it for publication was G. Durisi. *(Corresponding author: Francisco Sandoval.)*

F. Sandoval is with the Departamento de Ciencias de la Computación y Electrónica, Universidad Técnica Particular de Loja, Loja 11-01-608, Ecuador, and also with the Department of Electrical Engineering, École de Technologie Supérieure, Montreal, QC HC3 1K3, Canada (e-mail: fasandoval@utpl.edu.ec).

G. Poitau is the Chief Technology Officer, Ultra Electronics, TCS, Montreal, QC H4T 1V7, Canada (e-mail: gwenael.poitau@ultra-tcs.com).

F. Gagnon is with the Department of Electrical Engineering, École de Technologie Supérieure, Montreal, QC HC3 1K3, Canada (e-mail: francois.gagnon@etsmtl.ca).

Color versions of one or more of the figures in this paper are available online at http://ieeexplore.ieee.org.

Digital Object Identifier 10.1109/TCOMM.2019.2910811

Digital Video Broadcasting by Satellite (DVB-S), and Digital Video Broadcasting-Terrestrial (DVB-T). Moreover, the convolutional codes are the FEC codes for tactical communication such as Wideband Network Waveform (WNW) [10]. However, according to the knowledge of the authors, there is no extensive analysis of the choice of the convolutional codes parameters in relation to PAPR optimization.

PAPR reduction techniques based on codes such as SOPC, CBC, SBCC, and Golay Codes, are outside of the analysis made in this work and their comparisons with the formulation presented in this document is open for future work.

This paper is divided into five sections, including this introduction. Section II presents the Forward Error Correction (FEC) theory, the COFDM system model, the PAPR problem in a multicarrier system, and describes the distribution of PAPR for the COFDM system. Section III analyzes the autocorrelation characteristics of the COFDM based on a Markov Chain Model, and its relation to the peak factor of the COFDM signal. Additionally, this section introduces an upper bound on the peak factor of the COFDM signal, and its discussion for linear block codes and convolutional codes. The analysis of PAPR degradation in COFDM systems is reviewed in Section IV. Two cases are studied: the repetition code in Section IV-A and the convolutional codes based on the study of four important parameters: the code rate, the code structure, the maximum free distance, and the constraint length, in Section IV-B. The net gain concept is used in Section V to define the optimal convolutional code as a means to avoid an increase in the PAPR. In addition, the decoder complexity is discussed in Section V-A. The final section concludes the work.

II. Background

A. Forward Error Correction

Mobile channels are very hostile environments characterized by the presence of several noise sources such as white noise, impulse noise, echo, attenuation, intermodulation noise, and phase jitter. However, the real systems can be resolved successfully thanks to the inclusion in the systems of techniques such as the error control that permits robust transmission of data.

Forward error correction (FEC) is an error control method for data transmission where the transmitter adds redundant data to its messages with the objective of detecting and correcting errors without the need to re-transmit additional data. There are two main categories of FEC codes, depending on how redundancy is added, namely block codes and convolutional codes [11].

1) Block Codes: To construct a block code, we started by splitting the information sequence (for binary digits we have a binary block code) into 2^k message blocks of fixed length, with k information digits. The encoder mapped each input message into a coded word sequence of length η, where $\eta > k$. Hence, there were 2^k code words, and the rate of the code was k/η.

A linear block code $\mathcal{C}$ consists of a set of M code words (vectors) of length η denoted by $\mathbf{c}_m = (c_{m1}, c_{m2}, \cdots, c_{m\eta})$, $1 \leq m \leq M$, where for any two code words $\mathbf{c}_1$, $\mathbf{c}_2 \in \mathcal{C}$, we have $\mathbf{c}_1 + \mathbf{c}_2 \in \mathcal{C}$ [12].

In a linear block code, the transformation from information sequences, represented by a binary vector $\mathbf{u}_m$ of length k, to code words $\mathbf{c}_m$, can be given in matrix form by:

$$\mathbf{c}_m = \mathbf{u}_m \mathbf{G}, \quad 1 \leq m \leq 2^k, \tag{1}$$

where the matrix $\mathbf{G}$ of dimension $k \times \eta$ is the generation matrix. If a generation matrix of a linear block code is in the form of:

$$\mathbf{G} = [\mathbf{I}_k | \mathbf{P}], \tag{2}$$

we have systematic coding. In equation (2), $\mathbf{I}_k$ represents a $k \times k$ identity matrix and $\mathbf{P}$ is the parity matrix of dimension $k \times (\eta - k)$ [12].

Examples of block error correction codes are Repetition Codes, Hamming Codes, Reed-Solomon (RS) Codes, Bose-Chaudhuri-Hocquenghem (BCH) Codes, Golay Codes, and Low-Density Parity Check (LDPC) Codes.

2) Convolutional Codes: Unlike the block code, the convolutional code (CC) contains memory, i.e., the encoder output depends on the current and the previous input bits, Hence, a convolutional code can be easily implemented using a linear finite state shift register, and it can be characterized by three parameters (η, k, V), where η represents the code word length, k the input length, and the constraint length V is given by the number of bits stored in each shift register, plus the current input bits. So, similar to linear block codes, the code rate is given by k/η.

Although coding a convolutional code is a simple task, its decoding is much more complex. There are several proposed algorithms for decoding and one of the most known is the Viterbi algorithm (VA) which is an optimal algorithm (maximum-likelihood).

The VA calculates the distance (measure of similarity) between the received signal and all the trellis paths entering each state at a specific time. The Viterbi algorithm removes the trellis paths that can not be used by candidates for the maximum likelihood choice [13]. To remove, the VA, it chooses the path with the minimum metric between two paths that enter the same state, the path chosen is called surviving path [13]. The selection of surviving paths is made for all states.

There are two approaches to perform decoding namely hard decision decoding that receives a simple bitstream on its input, and the soft decision decoding [12].

The implementation of the VA consists of three main parts: the branch metric (BM) calculation, the path metric (PM) calculation, and the trace back (TB) operation. The branch metric is a measurement of the distance between the information transmitted and received. In the case of a hard decision decoding, the BM is the Hamming distance between the expected parity bits and the received ones. For a soft decision decoder, a BM is measured using the Euclidean distance. The PM is the sum of metrics of all branches in the path. For every encoder state, the path metric calculation calculates a metric for the survivor path ending in this state. Meanwhile, trace back is an operation used for hardware implementations that allows for the reduction of the information that must be stored in respect of the survivor's paths.

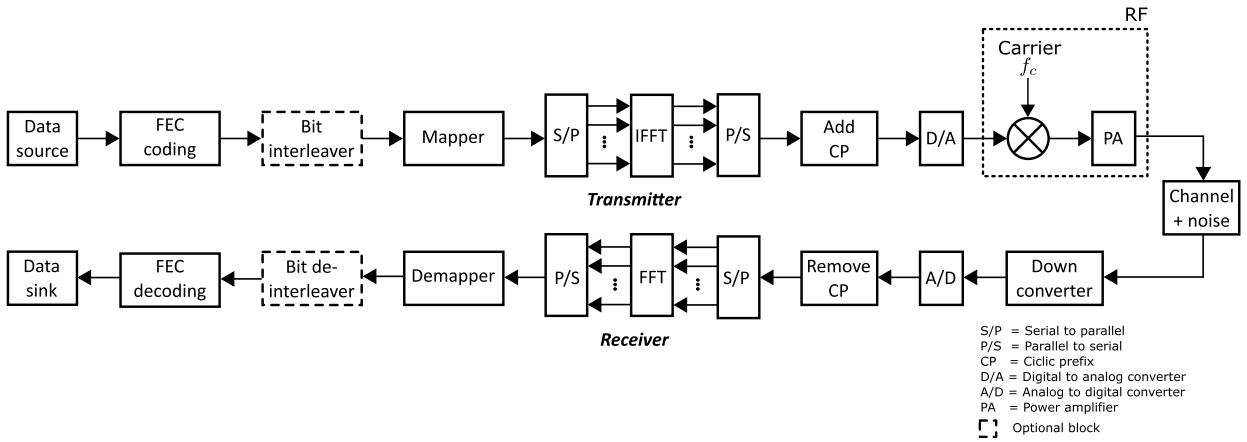

Fig. 1. Block diagram of transmitter and receiver in a coded OFDM system.

B. COFDM System Model

OFDM is a digital multiplexing and modulation technique that can be easily implemented due to the IFFT. If we consider N IFFT points, $\{X[l]\}_{l=0}^{N-1}$ represents the frequency-domain signal, where l is the frequency index. The discrete-time baseband OFDM signal $x[n]$ after applying IFFT is given by

$$x[n] = \frac{1}{\sqrt{N}} \sum_{l=0}^{N-1} X[l] e^{\mathrm{j}2\pi \frac{ln}{\mathcal{L}N}}, \quad n = 0, 1, \ldots, \mathcal{L}N - 1, \tag{3}$$

where n denotes the discrete-time index, j is the imaginary unit, and $\mathcal{L}$ is the oversampling rate.

The typical COFDM transmitter and receiver are presented in Fig. 1. First, the input information source is transformed into a sequence of channel symbols (code symbols) by the FEC coding block where one block code or convolutional code method can be used. Generally, on fading channels, the channel coding is combined with an interleaving block to mitigate the effect of error bursts [14, p. 267]. The bit interleaver block reorders the code symbols aiming at spreading out the burst errors. There are two main forms of interleaver: a block structure or a convolutional structure [12]. Next, the interleaver symbols or code symbols (when bit interleaver is not used) are mapped using a phase shift keying (PSK) or quadrature amplitude modulation (QAM). To generate the OFDM symbol, the input signal is serial-to-parallel (S/P) converter followed by an inverse fast Fourier transformer (IFFT). The OFDM symbol is parallel-to-serial (P/S) converter, a cyclic prefix (CP) of length N_{cp} is added, and the output is processed by the digital-to-analog (D/A) converter. Finally, the signal is prepared by the RF components to be transmitted through for the channel. At the receiver's end, the reverse process is performed.

C. PAPR Problem

A high peak to average power ratio (PAPR) can appear in the discrete-time OFDM signal when the N independent data symbols modulated on the N orthogonal subcarriers are added to the same phase. The PAPR in terms of discrete-time baseband OFDM signal can be written as:

$$\mathrm{PAPR}(x[n]) \triangleq \frac{\max\limits_{0 \le n \le N-1} |x[n]|^2}{\frac{1}{N} \sum\limits_{n=0}^{N-1} |x[n]|^2}. \tag{4}$$

D. Net Gain

In order to determine an appropriate FEC code to avoid increasing the PAPR, it is important to consider a global gain (net gain) in the system. In this work, the net gain is defined as a particular case of the fitness function-based approach [15], where two factors of interest are considered: the PAPR reduction and the BER performance. Hence, under given channel conditions (AWGN or multi-path), the relative PAPR reduction can be written as:

$$Y_1 = -10 \log_{10} \left(\frac{\mathrm{PAPR}_{\text{after}}}{\mathrm{PAPR}_{\text{before}}} \right), \tag{5}$$

and if we consider a certain signal to noise ratio (SNR) level, the relative degradation in BER performance is given by

$$Y_2 = -10 \log_{10} \left(\frac{\mathrm{BER}_{\text{after}}}{\mathrm{BER}_{\text{before}}} \right). \tag{6}$$

So, if α_u represents the weights of factors related to the significance level of PAPR reduction ($u = 1$), and BER ($u = 2$) in the system, the aggregate fitness value is [4]

$$\Gamma = \sum_{u=1}^{2} \alpha_u \cdot Y_u, \tag{7}$$

where

$$\sum_{u=1}^{2} \alpha_u = 1, \tag{8}$$

E. Distribution of the PARP for COFDM Signal

The complementary cumulative distribution function (CCDF) of PAPR represents the probability that the peak to average power ratio of the OFDM signal exceeds a given threshold γ (also represented by $\mathrm{PAPR0}$), i.e.

$\Pr(\text{PAPR} > \gamma)$. The CCDF is an important performance measure for evaluating PAPR reduction techniques, and we can use it to determine an appropriate value for the output back-off of a high power amplifier (HPA) [16].

A widely used simple approximation of the CCDF, is obtained based on the central limit theorem. Considering this principle, the real and imaginary parts of the time domain signal follow a Gaussian distribution with zero as the mean and a variance equal to 0.5 [2]. Therefore, in this case, the amplitude and power of the OFDM signal can be represented by a Rayleigh and chi-square distribution, respectively [2].

On the other hand, in [16], the extremal value theory of Gaussian random processes is used to achieve an accurate approximation for the CCDF of a bandlimited uncoded OFDM signal equal to:

$$\Pr(\text{PAPR} > \gamma) \cong 1 - \exp\left\{-Ne^{-\gamma}\sqrt{\frac{\pi}{3}\log N}\right\}. \quad (9)$$

In a practical implementation of the OFDM system there are three types of subcarriers namely data, pilot and null subcarriers. These subcarriers are allocated with unequal transmission power in order to make efficient use of limited power [17]. Based on that, more sophisticated CCDF expression derived by the aid of the Extreme Value Theory for Chi-squared-2 process for adaptive OFDM systems with unequal power allocation to subcarriers is given by [16] as

$$\Pr(\text{PAPR} > \gamma) \approx 1 - \exp\left\{-2e^{-\gamma}\sqrt{\frac{\pi\gamma\sum_{l=-L}^{L} l^2\sigma_l^2}{\sum_{l=-L}^{L}\sigma_l^2}}\right\} \quad (10)$$

where σ_l^2 denotes the transmission power allocated to the l-th subcarrier, $L = N_{\text{active}}/2$ if the subcarrier at DC is inactive; otherwise $L = (N_{\text{active}} - 1)/2$ if the DC subcarrier is active, N_{active} represents the active subcarriers (data subcarriers and pilot subcarriers), N_{inactive} corresponds to the inactive subcarriers (null subcarriers). Hence, the total number of subcarriers is $N = N_{\text{active}} + N_{\text{inactive}}$.

As highlighted by Jiang *et al.* [17] the PAPR distribution in OFDM systems is strongly impacted by the transmission power allocation. The expression in (10) is a general PAPR distribution and is valid for both cases where it is assumed that equal power is allocated to active subcarriers, and for the case with unequal power allocation to each subcarriers. In the first case with equal power allocated to the active subcarriers, $\sigma_l^2 = \rho P_{\text{av}}$, where $0 \leq \rho \leq N/N_{\text{active}}$, and P_{av} is the average power of the OFDM signal. Throughout this work, we assume equal power allocation to each active subcarrier to be $\rho = 1$.

Additionally, [16] considered the COFDM signal restricted to the case of codes that can be represented as uncorrected, and we demonstrated that the distribution of PAPR can be modeled by (9). The uncorrelated condition for forward error correction codes is met for many of the currently used codes, including, for instance, block codes (except repetition codes, and low rate codes [18, p. 527]), some convolutional codes, and turbo codes.

The question, therefore, is whether it possible to establish the behavior of PAPR distribution in the case where uncorrelated codes are used. We discuss this important question below, based on the relation between the autocorrelation and the maximum PAPR of the COFDM.

III. Autocorrelation Characteristics of COFDM Signal

In this section, we present a study about the autocorrelation before the IFFT block in an uncoded and in a coded OFDM system, and its relation to the CCDF of PAPR. In the case of COFDM, we propose that the Markov Chain Model is used, as given in [19], to calculate the autocorrelation function of the coded sequence, and we analyze some characteristics of the forward error correction codes that affect the PAPR.

A. Autocorrelation Characteristics of Uncoded OFDM Signal

In an uncoded OFDM signal, the autocorrelation function for the frequency-domain signal, $X[l]$, is defined by:

$$\rho[l] = \sum_{n=1}^{N-l} X[n+l]\cdot X^*[n] \quad \text{for } l = 0, \cdots, N-1. \quad (11)$$

An interesting relationship that depends only on the data sequence is highlighted in [20], between the autocorrelation of the IFFT input and the maximum PAPR of the uncoded OFDM signal, and can be given by:

$$\text{PAPR} \leq \Lambda = 1 + \frac{2}{N}\sum_{l=1}^{N-1} |\rho[l]|, \quad (12)$$

which describes an upper bound on the peak factor of the uncoded OFDM signal and provides a good approximation. Note that, based on (12), for the PAPR of the OFDM signal to be small, the values of the autocorrelation coefficients of the input sequences be small as well [21]. Therefore, this is not a necessary condition [21]. To compare the CCDF of PAPR of different OFDM signals, the autocorrelation can thus not be the only metric.

B. Markov Chain Model for Autocorrelation of Coded OFDM

The analytical expression for the autocorrelation function of typical code words with length η can be calculated based on a Markov Chain Model [19], [22]. Let s_i be the state at time t, and s_j, the state at the next time $t+1$ with $i = 0, \cdots, K-1$, and $j = 0, \cdots, K-1$. Each state s_i has an associated output code word vector $\mathbf{c}_i = [c_i(0), \cdots, c_i(\eta - 1)]$. We assume a *Mealy machine*; also known as a *finite-state synchronous sequential machine*, i.e., the output code word is a function of the current state only [19]. This represents a general assumption, and as will be shown in the following sections, multiple forward error correction codes can be represented by this model, both linear block codes such as repetition codes, systematic Hamming codes, and Reed-Solomon (RS) codes; as well as convolutional codes. Then, the complete statistics of

the stationary processes are given by the transition probability matrix, $\mathbf{\Pi} \triangleq [p_{ij}]_{K\times K}$, where p_{ij} are the probabilities of the transition from state s_i to state s_j. Additionally, we can define the state correlation matrix by the expression:

$$\mathbf{R}(k) = \begin{cases} \mathbf{D}\mathbf{\Pi}^k, & k \geq 0 \\ (\mathbf{\Pi}^H)^{-k}\mathbf{D}, & k < 0, \end{cases} \tag{13}$$

where the powers of $\mathbf{\Pi}^k$ are the $k-$step transition probability matrix. In equation (13), $\mathbf{D} = \text{diag}(p_0, \cdots, p_{K-1})$ is a diagonal matrix, where p_i for $i = 0, \cdots, K-1$ represents the steady-state probabilities of states s_i, and we can summarize these probabilities in the vector $\mathbf{p} = [p_0, \cdots, p_{K-1}]$. Another important matrix for which we need to define the autocorrelation is:

$$\mathbf{C} = \begin{bmatrix} c_0(0) & \cdots & c_0(\eta-1) \\ \vdots & \ddots & \vdots \\ c_{K-1}(0) & \cdots & c_{K-1}(\eta-1) \end{bmatrix}, \tag{14}$$

that has the K code words $\mathbf{c}_i$ corresponding to the K states s_i.

The discrete autocorrelation function of the coded sequence can be defined when we know the state transition matrix and all the possible code words and is given by [19]:

$$\rho[j] = \sum_k \sum_i \mathbf{c}^H(i)\mathbf{R}(k)\mathbf{c}(i+j-\eta k) \tag{15}$$

where $0 \leq i \leq \eta - 1 \cap 0 \leq i + j - \eta k \leq \eta - 1$ describes the ranges of i and k. In equation (15), $\mathbf{c}(i) = [c_0(i), \cdots, c_{K-1}(i)]^T$ is a column vector of the matrix $\mathbf{C}$, and $\mathbf{R}(k)$ represents the state correlation matrix defined in (13).

C. Upper Bound on Peak Factor of Coded OFDM Signal Analysis

In Section III-A, we present an upper bound on the peak factor of the OFDM signal. Next, in Section III-B, we describe a method for computing the autocorrelation function of a coded OFDM sequence. If we substitute (15) into (12), we can define an upper bound on the peak factor of a coded OFDM signal, and some characteristics that may limit the increase of PAPR in a coded OFDM system can be established.

We then study a particular case in relation to the FEC code used in the OFDM system, first, with a linear block code, and next with a convolutional code.

1) Linear Block Code: In the case of linear block codes, the Markov model is simple because, if we consider an $L-$ary code, all the transition probability from state s_i to state s_j are equal to $1/K$, where $K = L^M$ represents the number of states; i.e., the transition probability matrix can be given by [19]:

$$\mathbf{\Pi} = \begin{bmatrix} 1/K & \cdots & 1/K \\ \vdots & \ddots & \vdots \\ 1/K & \cdots & 1/K \end{bmatrix}, \tag{16}$$

Moreover, the steady-state probabilities $p_i = 1/K$ for all $i = 0, \cdots, K-1$. Hence, the diagonal matrix $\mathbf{D}$ is computed as [19]:

$$\mathbf{D} = \text{diag}(1/K, \cdots, 1/K). \tag{17}$$

So, the state correlation matrix is reduced to [19]:

$$\mathbf{R}(k) = \begin{cases} \mathbf{D}, & k = 0 \\ \mathbf{D}\mathbf{\Pi}, & \text{otherwise.} \end{cases} \tag{18}$$

Finally, we can find the autocorrelation function of an encoded OFDM signal from (15). By replacing the values and simplifying (15), we get the following result:

$$\rho[j] = \begin{cases} \dfrac{1}{K} \cdot \displaystyle\sum_i \mathbf{c}^H(i) \cdot \mathbf{c}(i+j), & k = 0 \\ \dfrac{1}{K^2} \cdot \displaystyle\sum_k \sum_i \mathbf{c}^H(i) \cdot \mathbf{c}(i+j-\eta k), & \text{otherwise,} \end{cases} \tag{19}$$

Hence, when the number of states or code words K increases, the autocorrelation $\rho[j]$ decreases, and this can have an impact on the PAPR bound expressed in (12).

The autocorrelation functions for some examples of linear block codes are presented by Mannerkoski and Koivunen in [19], for instance, a systematic Hamming code with generation matrix $\mathbf{G} = [\mathbf{I}_4|\mathbf{P}]$, where the parity matrix is defined by

$$\mathbf{P} = \begin{bmatrix} 1 & 0 & 1 \\ 1 & 1 & 1 \\ 1 & 1 & 0 \\ 0 & 1 & 1 \end{bmatrix}, \tag{20}$$

is considered. In this case, the number of states and code words is equal to $K = 2^4$, and [19] demonstrated that the absolute value of the analytical $\rho[j]$ (equation (15)) of the encoded sequence is equal to the Dirac delta function $\delta(j)$, i.e., we have whiteness autocorrelation. However, there are other linear block codes where $\rho[j]$ is not perfectly white [19], and codes with colored autocorrelation, such as repetition codes [19], are present.

Repetition is a simple solution introduced in coding theory, where the idea is to repeat the message η times for transmission. For example, in the case of $\eta = 4$, the generation matrix is given by $\mathbf{G} = [1\ 1\ 1\ 1]$, and there are two states s_0 and s_1 associated to the symbols 0 and 1, i.e, $K = 2$ and $\mathbf{\Pi}$ is a (2×2) matrix with all elements equal to 1/2. Therefore, the column vector of the matrix $\mathbf{C}$ is $\mathbf{c}(i) = [-1\ 1]^T$ for all i, where $i = 0, \ldots, 3$, i.e., $\mathbf{C}$ is a matrix of dimension (2×4). The autocorrelation $\rho[j]$ can be computed by (15) and is presented in Fig. 2a, where it is possible to see that the repetition encoded sequence has colored autocorrelation. Additionally, the case is considered when $\eta = 8$. In this case, $\mathbf{C}$ is a matrix of (8×2) with the same columns given by $\mathbf{c}(i) = [-1\ 1]^T$ for $i = 0, \ldots, 7$, and the state correlation matrix $\mathbf{\Pi}$ is equal to that in the case of $\eta = 4$. The autocorrelation is given in Fig. 2b, and in this is intuitively clear that there is an increase in the autocorrelation when η increases.

Note that BPSK modulation has been used in the example of repetition code to find the matrix $\mathbf{C}$. BPSK is considered here to simplify the calculations, but under a similar procedure high modulations can be included in the demonstration. Besides, when mapper operation is considered in the $\mathbf{C}$ matrix, the autocorrelation of the coded sequence calculated by (15)

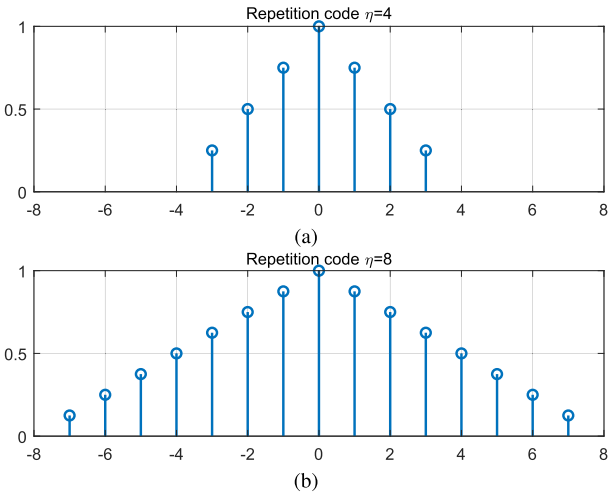

Fig. 2. (a) Autocorrelation of repetition code with $\eta = 4$, (b) Autocorrelation of repetition code with $\eta = 8$.

corresponds to the autocorrelation before the IFFT block in the COFDM system in Fig. 1; therefore, the calculated autocorrelation value allows finding the upper bound on the peak factor of the coded OFDM when (12) is used.

Another interesting example presented in [19] analyzes the Reed-Solomon (RS) Codes case, where it is important to highlight the large value for the number of code words and K states. For instance, with a $\eta = 7$, $M = 3$, and 8-QAM RS-code there are a total of $K = 8^3$, and for a $\eta = 15$, $M = 5$, and 16-QAM RS-code, there are $K = 16^5$ code words and states [19]. Therefore, when this large value of K is considered in the inverse relation presented in (19) between the autocorrelation and the number of code words and states, it is clear that the value of autocorrelation tends to white.

2) Convolutional Code: Consider the convolutional encoder (2, 1, 3) with generators given in octal form equal to [7, 5] (see Fig. 3a); thus, the code rate is $R = k/\eta = 1/2$, and the state diagram has $2^{k(V-1)}$ possible states (see Fig. 3b). On the other hand, the states of the Markov chair are defined by the register contents [19]. So, there are $K = 2^3$ possible states of the Markov chair, and 2^3 possible code words. Hence, the transition probability matrix is given by:

$$\mathbf{\Pi} = \begin{bmatrix} 1/2 & 0 & 0 & 0 & 1/2 & 0 & 0 & 0 \\ 1/2 & 0 & 0 & 0 & 1/2 & 0 & 0 & 0 \\ 0 & 1/2 & 0 & 0 & 0 & 1/2 & 0 & 0 \\ 0 & 1/2 & 0 & 0 & 0 & 1/2 & 0 & 0 \\ 0 & 0 & 1/2 & 0 & 0 & 0 & 1/2 & 0 \\ 0 & 0 & 1/2 & 0 & 0 & 0 & 1/2 & 0 \\ 0 & 0 & 0 & 1/2 & 0 & 0 & 0 & 1/2 \\ 0 & 0 & 0 & 1/2 & 0 & 0 & 0 & 1/2 \end{bmatrix}, \tag{21}$$

All states and the register content possibilities are presented in Table I. Unlike the linear block code in Section III-C1, when convolutional codes are used, the state transition matrix is not identical and the result is not general [19]. Moreover, we need the code word matrix $\mathbf{C}$ for the (2, 1, 3) convolutional code, which can be created based on the output of the convolutional

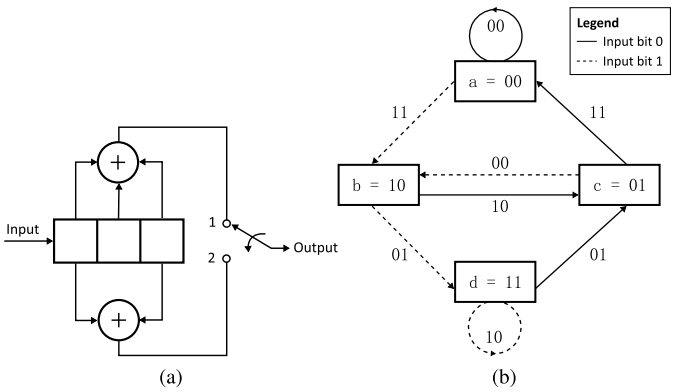

Fig. 3. (a) (2, 1, 3) convolutional encoder, (b) state diagram for (2, 1, 3) convolutional encoder [13].

TABLE I

REGISTER CONTENTS, OUTPUT CODE WORDS AND ELEMENTS OF THE CODE WORD MATRIX FOR CONVOLUTIONAL CODE (2, 1, 3)

State s_i	Register contents	Output	$\mathbf{C}$ elements
s_0	000	00	-1,-1
s_1	001	11	1,1
s_2	010	10	1,-1
s_3	011	01	-1,1
s_4	100	11	1,1
s_5	101	00	-1,-1
s_6	110	01	-1,1
s_7	111	10	1,-1

encoder presented in the third column of Table I for each state. The elements of the code word matrix are presented in the fourth column of the Table I and results of changing the output code words (third column) to obtain a zero-mean sequence in the output of the convolutional encoder [19], i.e., we change 0 by -1 and 1 by $+1$ (BPSK modulation, for simplicity).

The autocorrelation for the convolutional code can be found by the expression in (15), and similar to the example presented for repetition code, the upper bound on the peak factor is given by the substitution of the autocorrelation value in (12).

In some cases, e.g., a $\eta = 7$, $M = 3$, and 8-QAM Reed-Solomon code, computing the matrix $\mathbf{\Pi}$ is too expensive [19]. Therefore, we can estimate the autocorrelation by the expression [19]:

$$\hat{\rho}[j] = \frac{1}{N_s} \sum_{n=1}^{N_s} \left[w(n) w^*(n-j) \right], \tag{22}$$

where N_s is the number of samples and $w(n)$ the output of the convolutional encoder. This expression is used in this paper to find the simulation result in Section IV.

IV. ANALYSIS OF PAPR DEGRADATION IN COFDM

In this section, we present a validation of the concepts presented in Section III-B, based on the calculation of the CCDF of PAPR, the BER, and the autocorrelation of the signal before the IFFT block. First, in the case of linear block codes, for simplicity, we consider as an example, repetition codes with and without interleaving, and a simple variation called

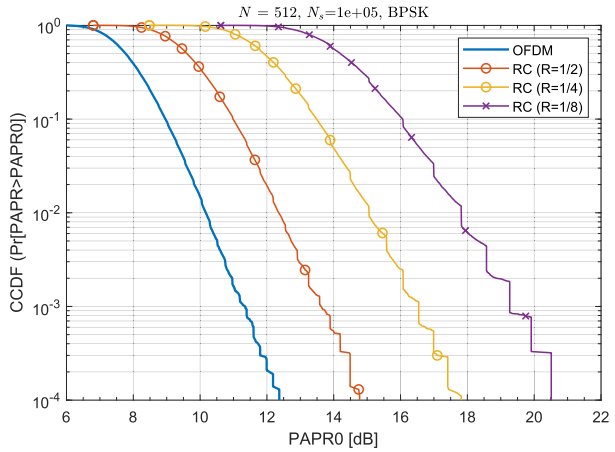

(a) CCDF

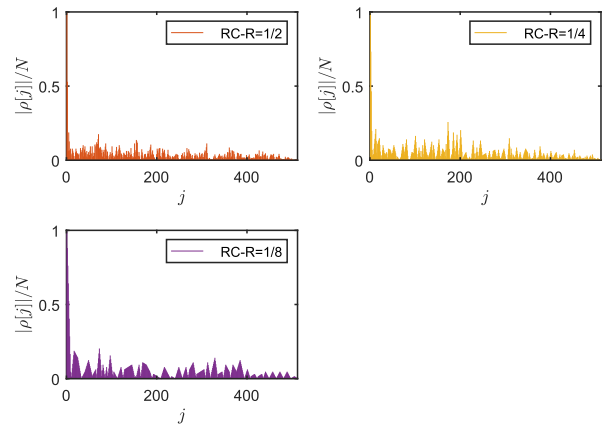

(b) Autocorrelation

Fig. 4. COFDM system with repetition code with code rate 1/2, 1/4, and 1/8, $N = 512$ subcarriers, and $N_s = 10^5$ OFDM symbols simulated.

a modified code repetition (MCR). Then, the influence of the convolutional codes is analyzed.

A. Linear Block Code: Repetition Code

The behavior of the autocorrelation in relation to the value of the CCDF of PAPR in a COFDM signal when using linear block codes is studied based on the use of repetition codes in the system.

In the case of repetition code, according to the analysis presented in section III-C1, we know that the variable parameter that affect the autocorrelation of the code word is the code rate R. Thus, it is also known that for the calculation of the autocorrelation through (15) both the matrix $\mathbf{\Pi}$ and $\mathbf{D}$ remain constant and the column vector $\mathbf{c}(i)$ is identical for all i, but the number of columns of the matrix $\mathbf{C}$ changes according to η which, as shown in Fig 2, can modify the autocorrelation. The impact of code rate over the autocorrelation and the CCDF in COFDM signal is analyzed in Fig. 4 where the CCDF of PAPR of COFDM signals with repetition codes (RC) for different code rate value is plotted (see Fig. 4a). The reference is the OFDM signal and a BPSK modulation is used for all cases. Also, Fig. 4b shows the autocorrelation for repetition code with code rates 1/2, 1/4 and 1/8, and based on these, the value of the upper bound peak factor Λ for repetition code with $R = 1/2$, 1/4, and 1/8 is 15.4629 dB, 16.8448 dB, and 17.4570 dB, respectively. Therefore, it is possible to see that the reduction of the code rate for a repetition code, can increase the autocorrelation, and also the PAPR of COFDM system.

As we have seen, the use of repetition codes generates colored autocorrelation. To achieve an autocorrelation closer to white, we also tested the use of a repetition code plus a block interleaver. The block interleaver used in this work writes across rows in the input and reads down columns in the output. Additionally, we evaluated the use of the modified code repetition (MCR) technique presented in [23], which allows a reduction of the peaks for a BPSK OFDM signal. Ngajikin *et al.* [23] suggested using a repetition code and modified the last bit of the word, by toggling up. For example, for $k = 4$ number of repetitions, the input bit 0 produces the output $'0000'$ when code repetition is used, and in the case of MCR, the output will be $'0001'$. Two code rates are analyzed: $R = 1/4$, and $R = 1/8$.

The CCDF of PAPR of the COFDM signals with repetition codes (RC), repetition codes plus interleaver (RC + Int), and MCR plus interleaver (MCR + Int), for BPSK and QPSK modulation are show in Fig. 5a for code rate 1/4, and in Fig. 6a for code rate 1/8. Also, the conventional OFDM with BPSK and QPSK modulation is added for comparison. With code rate 1/4, the use of a repetition code with QPSK presents a large value of PAPR, and compared to conventional OFDM BPSK signal, MRC plus interleaver with BPSK slight decrease can be achieved. On the other hand, the BER performance for the OFDM signal plus RC, RC + Int, and MRC + Int with code rates 1/4 and 1/8 are presented in Fig. 5b, and Fig. 6b, respectively. For same BER value, the better SNR are given for the MRC + Int and RC + Int than RC alone. Meanwhile, Fig. 5c and Fig. 6c show the autocorrelation for all cases with code rates 1/4 and 1/8, respectively. In the cases analyzed, the OFDM signal with repetition code presents a large value of autocorrelation and a large value of PAPR. Finally, the value of the upper bound peak factor Λ for repetition code, repetition code plus interleaver, and MCR plus interleaver for BPSK and QPSK modulation with code rates 1/4 and 1/8 is presented in Table II.

B. Convolutional Codes

If a convolutional code is used in the COFDM system, the autocorrelation, and consequently, the PAPR of the OFDM signal, depends on the code word, i.e., the code rate, the code structure, and the state correlation matrix that is related to the constraint length V. On the one hand, it is known that lower code rate leads to better performance. However, a more powerful code leads to extra redundancy and less bandwidth efficiency. On the other hand, more coding gain and more powerful convolutional code are obtained when a longer constraint length is used. However, the larger constraint length leads to more complex decoder and more decoding delays [12].

Below, we study in more detail these important parameters, i.e., the code rate R, the code structure, and the constraint

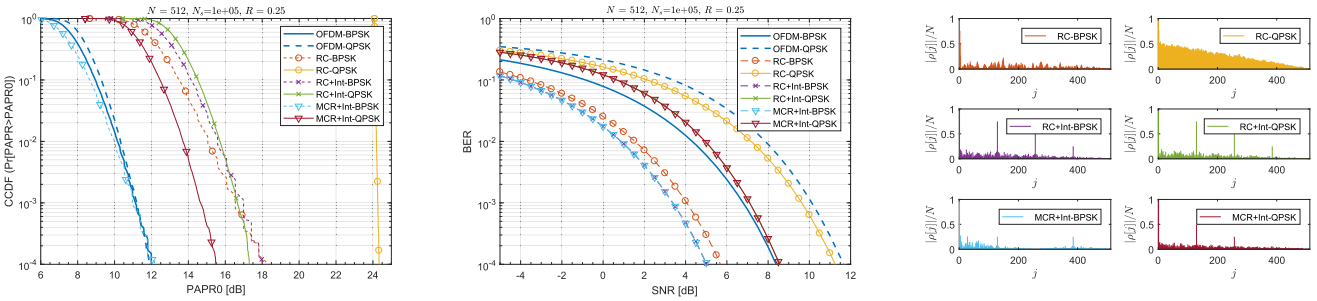

(a) CCDF (b) BER (c) Autocorrelation

Fig. 5. COFDM system with repetition code, repetition code plus interleaving and MCR plus interleaving with code rate 1/4, $N = 512$ subcarriers, and $N_s = 10^5$ OFDM symbols simulated.

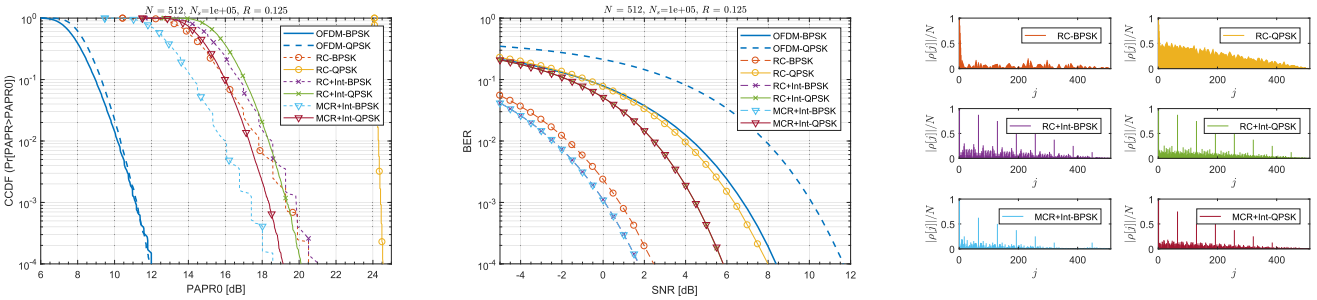

(a) CCDF (b) BER (c) Autocorrelation

Fig. 6. COFDM system with repetition code, repetition code plus interleaving and MCR plus interleaving with code rate $R = 1/8$, $N = 512$ subcarriers, and $N_s = 10^5$ OFDM symbols simulated.

TABLE II

Λ FOR COFDM USED IN THE LINEAR BLOCK CODE EXAMPLES

Code Rate (R)	Code	Modulation	Λ (dB)
1/4	RC	BPSK	16.5170
1/4	RC	QPSK	24.0986
1/4	RC+Int	BPSK	15.8130
1/4	RC+Int	QPSK	16.4278
1/4	MCR+Int	BPSK	13.9808
1/4	MCR+Int	QPSK	15.7127
1/8	RC	BPSK	17.0850
1/8	RC	QPSK	24.0916
1/8	RC+Int	BPSK	17.4964
1/8	RC+Int	QPSK	18.1708
1/8	MCR+Int	BPSK	14.8961
1/8	MCR+Int	QPSK	16.8202

length V, and we analyze how they affect the PAPR of an OFDM signal. This can be an important point to take into account when designing an encoder. Also, we include in the discussion the maximum free distance Convolutional codes in case of code rates 1/2, 1/4 and 1/8 and compare its CCDF of PAPR, its BER, and its autocorrelation. In all simulations for the case of convolutional codes in this section, we consider an OFDM signal with $K = 256$ subcarriers, a guard interval percentage equal to 25%, a quadrature phase-shift keying (QPSK), and an oversampling rate $\mathcal{L} = 1$. An additive white Gaussian noise (AWGN) channel is assumed, and the receiver uses a hard Viterbi decoder with memory truncation and traceback depth defined by $2.5 \cdot [(V-1)/(1-R)]$ [24]. The algorithm is executed $N_s = 10^5$ times in each case.

1) Code Rate: Considering a forward error correction (FEC) code, the code rate is the proportion between the length of information digits and the length of the code word sequence. For instance, if the code rate is equal to 2/3, then for each three bits, two correspond to data, and one is a redundancy. Typical convolutional code rate values are 1/2, 1/4, 1/8, 2/3, 3/4, 5/6 and 7/8.

A study examining the influence of the code rates of nonrecursive nonsystematic convolutional codes on the peak degradation of the COFDM signal is presented in [25], where it is concluded that the PAPR can be increased in the case of a code rate $R < 1/2$ and relatively low constraint lengths $V = 3$ through $V = 6$ [25]. This conclusion is based on simulation results only.

Consider three convolutional codes with code rate 1/2, 1/4 and 1/8, similar constraint length $V = 3$, and without a significant structure defined by the polynomials in octal form: [5, 7], [1, 3, 7, 3], and [1, 5, 7, 3, 1, 5, 3, 7], respectively. For all three cases, there are $K = 2^3$ possible states of the Markov chain, and the same possible code words. The transition probability matrix is given by (21) and all states, register contents, and output possibilities are presented in Table III. The code word matrix $\mathbf{C}$ is obtained from Table III for each code word by the application of a BPSK mapped to the output when each code word is used. Therefore, the resulting code word matrices $\mathbf{C}$ has dimensions of (8×2), (8×4), and (8×8) for $R = 1/2$, 1/4, and 1/8, respectively. Thus, in the case of constant constraint length, the autocorrelation changes according to the code word matrix. In this case, when analyzing the first two

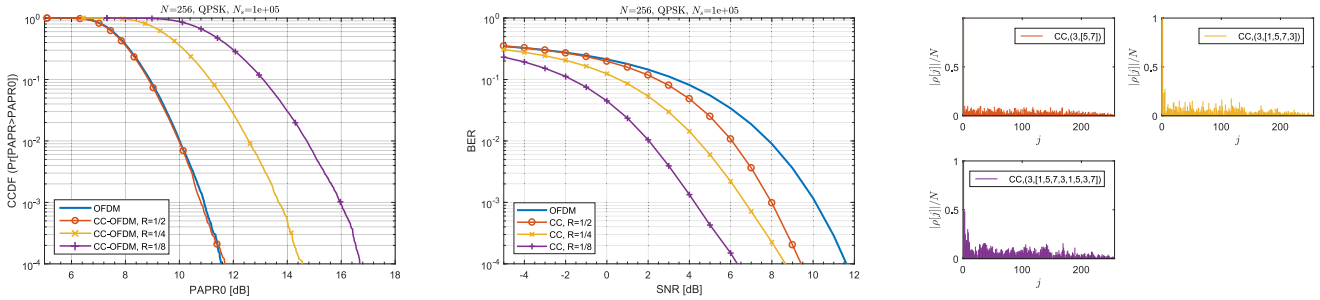

(a) CCDF (b) BER (c) Autocorrelation

Fig. 7. COFDM-QPSK system for different convolutional code rate with $N = 256$ subcarriers, and $N_s = 10^5$ OFDM symbols simulated.

TABLE III

STATES, REGISTER CONTENTS, AND OUTPUT CODE WORDS FOR CONVOLUTIONAL CODES: $(V = 3; [5, 7])$, $(V = 3; [1, 3, 7, 3])$, AND $(V = 3; [1, 5, 7, 3, 1, 5, 3, 7])$

		Output		
State s_i	Register contents	[5, 7]	[1, 3, 7, 3]	[1, 5, 7, 3, 1, 5, 3, 7]
s_0	000	00	0000	00000000
s_1	001	11	1111	11111111
s_2	010	01	0111	00110011
s_3	011	10	1000	11001100
s_4	100	11	0010	01100101
s_5	101	00	1101	10011010
s_6	110	10	0101	01010110
s_7	111	01	1010	10101001

states for the three examples cases, we can observe an output similar to that in the example presented with repetition code. So the autocorrelation increases, in these cases, when the code word decrease, as analyzed in Fig. 2. Although this conclusion is based on a particular example, it is intuitively clear, that there are more options to have states that generate long chains of repetition at the output when the code rate decreases.

The CCDF of PAPR (see Fig. 7a), and the BER (see Fig. 7b) of the COFDM signals with convolutional codes [5, 7], [1, 3, 7, 3], and [1, 5, 7, 3, 1, 5, 3, 7] are calculated. We can see that the code rate decrease may increase the PAPR in the COFDM signal. In this example, only the polynomial [5, 7] corresponds to a maximum free distance code. For instance, in the example proposed here, the convolutional code OFDM signal with code rate 1/2 (see curve CC-OFDM, $R = 1/2$ in Fig. 7a) has a similar CCDF of PAPR as the OFDM signal. However, the curves with code rates 1/4 and 1/8 (see curves CC-OFDM, $R = 1/4$, and CC-OFDM, $R = 1/8$ in Fig. 7a, respectively), when the CCDF is equal to 10^{-4} lose 3.2, and 5.1 dB, respectively, in the PAPR as compared to the OFDM signal. Meanwhile, the BER curves; (Fig. 7b) report the expected behavior when using different code rates. Next, the normalized value of absolute autocorrelation of the COFDM signals with convolutional codes represented by the polynomials [5, 7], [1, 3, 7, 3], and [1, 5, 7, 3, 1, 5, 3, 7] is presented in Fig. 7c. Additionally, the value of the upper bound on the peak factor Λ described in (12), based on the autocorrelation calculated in Fig. 7c is calculated. For the case of code rate $R = 1/2$, 1/4, and 1/8 the upper bound on the peak factor (Λ) is 12.7012 dB, 13.8997 dB, and 15.5053 dB, respectively.

2) Code Structure: There are many code structures that can be used to generate the convolutional code; however, each code structure differs in its results in terms of error detection and error correction capabilities, and can also generate different values of PAPR for the system. For example, Frontana and Fair [25], through simulation results, suggest that a significant structure in the convolutional encoder can lead to a degradation in the PAPR because it may cause a constructive summation on many of the subcarriers [25].

We consider that a convolutional code has a significant structure if at least two consecutive bits of the resulting code word is obtained by the same generator (this means that we get same bits in these positions). For example, in the convolutional code ($V = 3$; [5,7,7,7]) with code rate $R = 1/4$ the last three bits of each 4-bit code word are identical.

To quantify the effect of the significant structure of the convolutional code in the autocorrelation of the code word, we define the structure number (ς) as the number of consecutive generators existing in the generation of the code. For instance, the structure number for the convolutional code $V = 3$; [5,7,7,7] is $\varsigma = 3$.

The effect of the convolutional code structure on the value of autocorrelation is analyzed below. We consider four different polynomials, with a similar code rate $R = 1/4$, and constraint length $V = 3$, described in octal form by: [1, 3, 5, 7], [5, 5, 7, 7], [5, 7, 7, 7], and [7, 7, 7, 7] with structure number equal to $\varsigma = 1$, $\varsigma = 4$, $\varsigma = 3$, and $\varsigma = 4$, respectively. Again, $K = 3$, and the transition probability matrix is given by (21). All states, register contents, and output possibilities are presented in Table IV. The code word matrix has a dimension of (8×4) and it is constructed, with each output, by mapping $0 \rightarrow -1$ and $1 \rightarrow +1$. When analyzing the outputs in Table IV, it is possible to see that the repetition increases when the significant structure in the convolutional code also increases.

The effect is calculated by simulating the PAPR (Fig. 8a), the BER (Fig. 8b) and the absolute value of its autocorrelation (Fig. 8c); in a COFDM system with QPSK modulation. It can be concluded from the results that when a significant structure is presented in the convolutional code, the absolute value of the autocorrelation increases, and consequently, may produce a PAPR increase. For this example, it was observed that when the value of the structure number (ς) increased,

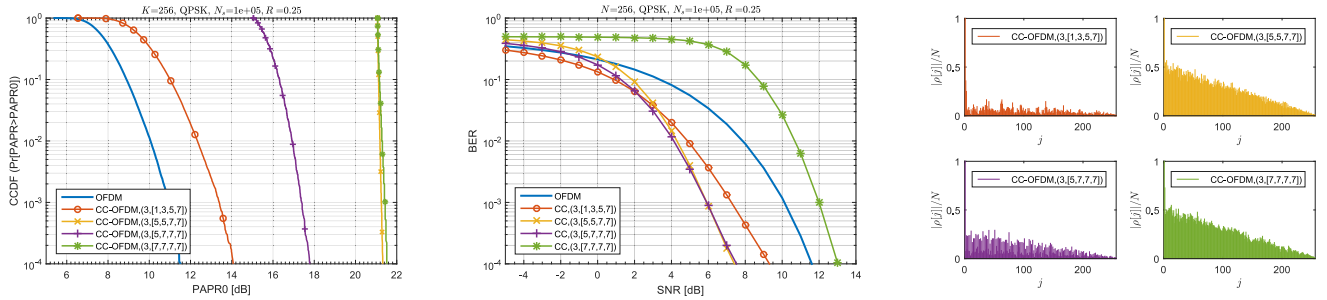

(a) CCDF (b) BER (c) Autocorrelation

Fig. 8. COFDM-QPSK system for different convolutional code structures with code rate $R = 1/4$, $N = 256$ subcarriers, and $N_s = 10^5$ OFDM symbols simulated.

TABLE IV

STATES, REGISTER CONTENTS, AND OUTPUT CODE WORDS FOR CONVOLUTIONAL CODES: $(V = 3; [1, 3, 5, 7])$, $(V = 3; [5, 5, 7, 7])$, $(V = 3; [5, 7, 7, 7])$, AND $(V = 3; [7, 7, 7, 7])$

State s_i	Register contents	Output			
		$[1, 3, 5, 7]$	$[5, 5, 7, 7]$	$[5, 7, 7, 7]$	$[7, 7, 7, 7]$
s_0	000	0000	0000	0000	0000
s_1	001	1111	1111	1111	1111
s_2	010	0101	0011	0111	1111
s_3	011	1010	1100	1000	0000
s_4	100	0011	1111	1111	1111
s_5	101	1100	0000	0000	0000
s_6	110	0110	1100	1000	0000
s_7	111	1001	0011	0111	1111

the autocorrelation and the PAPR also increased. For instance, if we consider the CCDF of PAPR equal to 10^{-4}, for $\varsigma = 1$ ([1, 3, 5, 7]) the PAPR is 14 dB, for $\varsigma = 3$ ([5, 7, 7, 7]) is 17.8 dB, and for $\varsigma = 4$ ([5, 5, 7, 7], and [7, 7, 7, 7]) are 21.3 dB and 21.5 dB, respectively. Regarding the BER results, it is important to highlight that only the polynomial [5, 7, 7, 7] is a maximum free distance code. The value of the upper bound peak factor Λ is equal to 14.3922 dB, 21.1666 dB, 16.31143 dB, and 21.1875 dB when the convolutional codes $(V = 3; [1, 3, 5, 7])$, $(V = 3; [5, 5, 7, 7])$, $(V = 3; [5, 7, 7, 7])$, and $(V = 3; [7, 7, 7, 7])$ are used in the COFDM system.

3) Maximum Free Distance Convolutional Codes: The free distance (d_{free}) is a minimal Hamming distance between different encoded sequences [12], and is related to the correcting capability of the code. In Table V the maximum free distance codes for code rates 1/2, 1/4, and 1/8 are presented.

The free distance is analyzed as a parameter here since the convolutional codes, with maximum free distance, represent the most used codes. In addition, the free distance impacts on the performance of the system. This effect will be included later in the calculation of the net gain and the convolutional code optimization.

In Fig. 9a, we present the CCDF of the PAPR for a selected group of maximum free distance codes in Table V. We can see in Fig. 9a that in the case of free distance convolutional codes with $R = 1/2$, all curves have the same response with respect to the CCDF of PAPR. However, when we consider the case with $R = 1/4$, the convolutional code $(V = 5; [25, 27, 33, 37])$ loses approximately 1 dB, and the codes $(V = 3; [5, 7, 7, 7])$ and $(V = 7; [135, 135, 147, 163])$ lose approximately 6 dB as

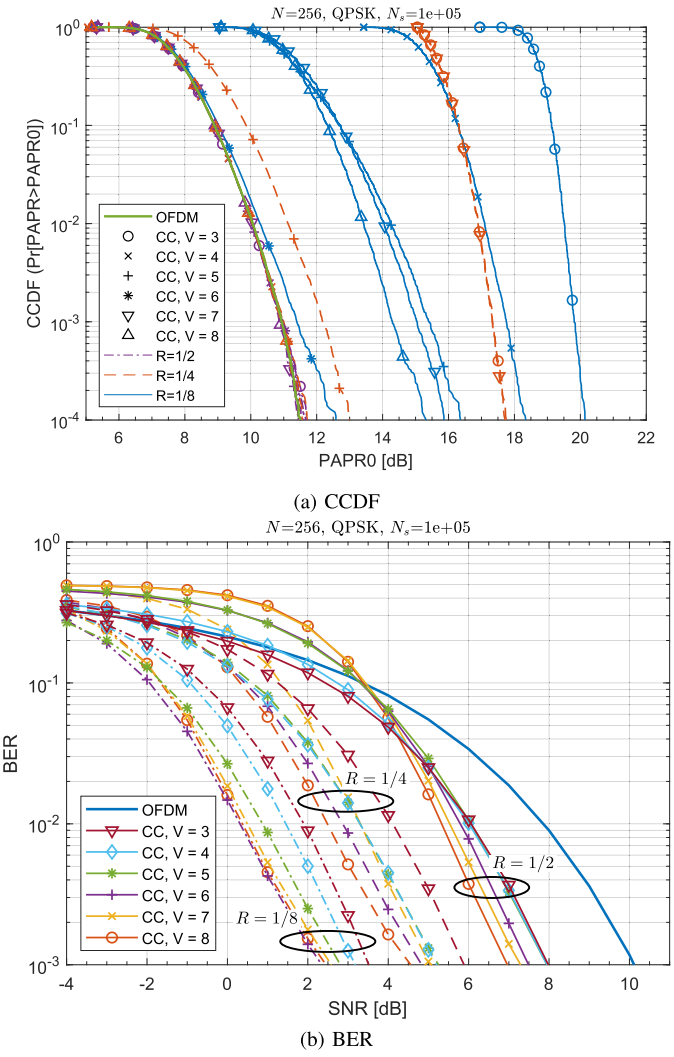

(a) CCDF

(b) BER

Fig. 9. COFDM-QPSK system for different maximum free distance convolutional codes with $N = 256$ subcarriers, constraint length V between 3 and 8, $N_s = 10^5$ OFDM symbols simulated, and code rates $R = 1/2$, $R = 1/4$, and $R = 1/8$.

compared to the OFDM signal. On the other hand, when the code rate is $R = 1/8$, all curves experience degradation. For instance, if we consider the CCDF of PAPR equal to 10^{-4}, the curve "CC, $V = 3$" loses 8.63 dB as compared with the OFDM curve. Similarly, the curve "CC, $V = 4$" loses 6.83 dB,

TABLE V

MAXIMUM FREE DISTANCE CODES [12] WITH CODE RATE 1/2, 1/4, AND 1/8, AND THE STRUCTURE NUMBER (ς) FOR EACH CODE

Constraint Length (V)	Rate 1/2				Rate 1/4						Rate 1/8									
	Generators in Octal		d_{free}	ς	Generators in Octal				d_{free}	ς	Generators in Octal								d_{free}	ς
3	5	7	5	1	5	7	7	7	10	3	7	7	5	5	5	7	7	7	21	8
4	15	17	6	1	13	15	15	17	13	2	17	17	13	13	13	15	15	17	26	7
5	23	35	7	1	25	27	33	37	16	1	27	33	25	25	35	33	25	25	32	4
6	53	75	8	1	53	67	71	75	18	1	57	73	51	65	75	47	67	57	36	1
7	133	171	10	1	135	135	147	163	20	2	153	111	165	173	135	135	147	137	40	2
8	247	371	10	1	235	275	313	357	22	1	275	275	253	371	331	235	213	357	45	2

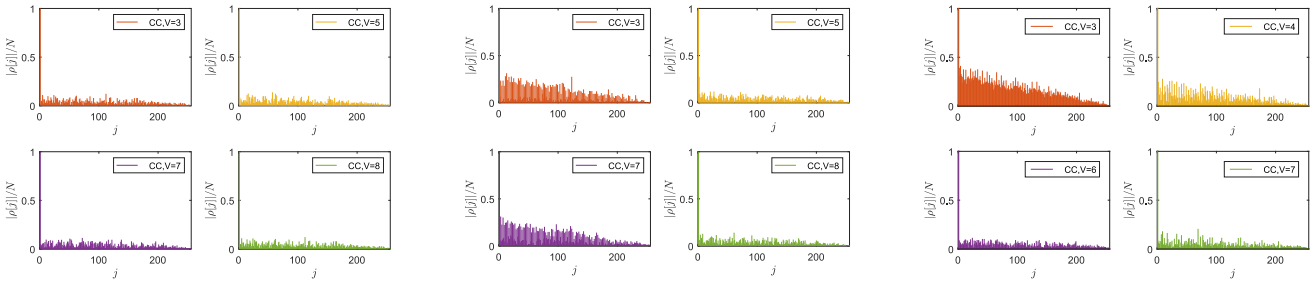

(a) $R = 1/2$ (b) $R = 1/4$ (c) $R = 1/8$

Fig. 10. Autocorrelation for COFDM-QPSK system with $N = 256$ subcarriers, $N_s = 10^5$ OFDM symbols simulated, different maximum free distance convolutional codes, and code rates $R = 1/2$, $R = 1/4$, and $R = 1/8$.

"CC, $V = 5$" loses 4.85 dB, "CC, $V = 6$" loses 1.07 dB, "CC, $V = 7$" loses 4.35 dB, and "CC, $V = 8$" loses 3.81 dB.

Table V presents the value of structure number ς for each generator. When the code rate is $R = 1/2$, all the generators show a structure number equal to 1 and all the codes experience same PAPR results. In the case of code rate $R = 1/4$ all the generators present $\varsigma = 1$ except for the codes with $V = 3$, $V = 4$, and $V = 7$. The code with constraint length $V = 3$ has the highest value of ς and the highest value of PAPR. The code with $V = 7$ that has $\varsigma = 2$ experience high value of PAPR, too. However, there is an exception in the case of $V = 4$, since it experiences a similar PAPR value as the reference OFDM signal although it has a value of $\varsigma = 2$. In contrast, the code with $V = 5$ with a value of $\varsigma = 1$, also has a value of PAPR greater than the reference signal OFDM. For codes with code rate $R = 1/8$ there is a direct relation between the increase of the structure number ς and that of the PAPR for all cases is observed.

Additionally, the BER for the maximum free distance codes with a constraint length between 3 and 8 are presented in Fig. 9b. Finally, we present the estimation of the normalized autocorrelation for four examples of each code rate in Fig. 10a, Fig. 10b, and Fig. 10c, respectively. The upper bound peak factor Λ for all possible cases is presented in Table VI.

4) Constraint Length: The constraint length parameter is linked to the possibility of having memory in the convolutional codes, i.e., if we consider one information bit in the input of the convolutional encoder, the constraint length represents the maximum number of encoder outputs that can be affected [26]. Frontana and Fair [25] demonstrated by simulation that in an OFDM system, the PAPR performance experiences

TABLE VI

Λ FOR COFDM USED FOR FREE DISTANCE CODE EXAMPLE

	Λ (dB)		
Constrain length (V)	R=1/2	R=1/4	R=1/8
3	12.8131	16.0999	19.1310
4	12.9730	12.4933	15.7781
5	12.9761	13.2805	13.4960
6	12.9150	13.1190	13.2172
7	13.0507	16.3264	13.3310
8	13.1398	13.0456	13.5317

degradation when the constraint length is low. To analyze the effect of the constraint length on the COFDM system, we consider the examples proposed in Section IV-B3.

For the proposed examples, the code rate can assume the values of 1/2, 1/4, and 1/8, while the constraint length varies between 3 to 8, and the structure number is a variable for the cases $R = 1/4$ and $R = 1/8$. Since, the constraint length is a variable, the matrices $\mathbf{\Pi}, \mathbf{D}$, and $\mathbf{C}$ are also variables as well as the number of states and possible code words that change in relation to $K = 2^V$.

In the case of code rate $R = 1/2$ (Fig. 9a), we can see that changes in constraint length do not affect the CCDF of PAPR performance. In the second example, with code rate 1/4 (Fig. 9a), the situation differs. The performance of the CCDF of PAPR in the COFDM system with convolutional codes, with $V = 3$, $V = 5$, and $V = 7$, is worse than for the OFDM system. However, it is important to highlight that the polynomial of convolutional codes with $V = 3$ and $V = 7$ present a significant structure as well. In example three, in the

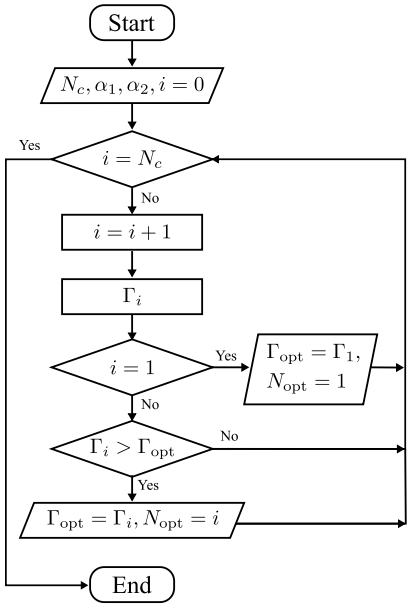

Fig. 11. Algorithm to calculate the optimal code to avoid an increase in the PAPR based on the net gain.

COFDM system with $R = 1/8$ (Fig. 9a), the behavior is different. All the polynomials experience losses, and we can see that when the polynomial with the least constraint length has worst CCDF of PAPR, except in the case of a polynomial with $V = 7$. In this case, the polynomial with $V = 6$, 7 and 8 do not have a significant structure. Therefore, in this case, the law that stipulates that the PAPR increases when the value of the constraint length decreases predominates.

V. Optimal Convolutional Code to Avoid an Increase in the PAPR Based on Net Gain

To define the optimal convolutional code of a given rate with a given constraint length, we use the net gain concept defined in Section II-D to compare all the maximum free distance codes for code rates 1/2, 1/4 and 1/8 presented in Table V. The procedure followed to obtain the optimal codes is presented in Fig. 11, where N_c is the number of codes to compare, Γ_{opt} is the optimal net gain for all codes, and N_{opt} is the optimal code chosen.

In addition, we need to provide a specific value for the CCDF of PAPR and the BER to make the net gain comparison. These values may vary for different services offered by a system. For example, in a multimedia connection, we can consider three components with different quality of service (QoS), such as voice, video, and packet data. For voice service, the error probably in the region of 10^{-3} is typical [27]. The video service has a greater sensibility to errors, and it regularly requires a BER in the region of 10^{-6} [27]. On the other hand, For the packet data communications, in the case of high-speed Internet access, acceptable BER is 10^{-9} [27]. In this work, a BER equal to 10^{-3} is used for net gain evaluation as in the case of digitized voice service [14, p. 181]. On the other hand, as shown in this case, a simulation is carried out using the Monte Carlo method, to generate a comparison with a reasonable uncertainty data when the observer value is $10^{-\varrho}$, leastwise $N_s = 10^{\varrho+1}$ bits are processed through the system which produces a confidence interval of about $(2\hat{p}, 0.5\hat{p})$, where $\hat{p}$ is the estimator of the BER [28].

In the case of the CCDF of PAPR, the typical values used in the literature for the comparison of PAPR reduction techniques are between 10^{-3} [2], [16] to 10^{-5} [29], so here 10^{-4} is used as a reference for net gain calculation.

If we change the reference value for the BER or the CCDF of PAPR, significant changes may occur in the result of the net gain, so it is advisable to perform the net gain calculation according to the application system.

Three cases of net gain were calculated: 1), when $\alpha_1 = \alpha_2 = 0.5$, i.e., equal importance for PAPR and BER improvement; 2), when $\alpha_1 = 0.75$ and $\alpha_2 = 0.25$, it is more important to achieve a reduced value of PAPR; and 3), when $\alpha_1 = 0.25$ and $\alpha_2 = 0.75$, it is more important to achieve BER improvement. The net results gain for different maximum free distance convolutional codes with code rates 1/2, 1/4 and 1/8 are shown in Table VII. We consider the basic OFDM system as a reference. A large value for the Y_1 implies a lower value of PAPR, and a large value for the variable Y_2 implies a better performance (less BER) as compared to conventional OFDM. ΔPAPR represents the variation between the PAPR value for OFDM signal and the COFDM signal at a specific value of CCDF. Similarly, ΔSNR is the variation between the SNR value for the reference signal and the COFDM signal at a specific value of BER.

The net gain calculated in the first case, $\alpha_1 = \alpha_2 = 0.5$, for code rates 1/2, 1/4 and 1/8 is presented in Fig. 12a, where it can be seen that in the case of code rate 1/2, the best options for the convolutional code are the code with constraint length $V = 8$. When the code rate is equal to 1/4, the worst results seen are for codes with constraint lengths 3, and 7, and the convolutional codes with constraint lengths 4, 6, and 8 have good performance. In the case of code rate 1/8, the best option is the convolutional code with constraint length 6. Based on these results, it can be affirmed that the best codes with maximum free distance codes for code rates 1/2, 1/4 and 1/8, with $\alpha_1 = \alpha_2 = 0.5$, are the codes with constraint lengths equal to 8, 8, and 6, respectively. The best net gain for each case is highlighted in gray in Table VII, VII.

Additionally, in Fig. 12b the variation of PAPR Y_1 (left axis), and the variation of BER performance Y_2 (right axis) in the case $\alpha_1 = \alpha_2 = 0.5$ is plotted for code rates 1/2, 1/4 and 1/8, and different values of constrain length (V).

Considering the left axis (Y_1), we can see that in the case of code rate 1/2, for different value of constraint length, slight differences are present. However, with the code rate equaling 1/4 or 1/8, differences in the PAPR of approximatively 6 dB for the case of R = $1/4$, or 8 dB in the case of code rate 1/8 are shown, between codes with different constraint length. The smallest PAPR is presented for cases with constraint length equal to 3 and 7 (R = $1/2$), 8 (R = $1/4$), and 6 (R = $1/8$). Besides, it can be seen that for all tested cases there are PAPR degradation; however, the system can be optimized through an accurate selection of the code which can lead to minimum increments for all cases.

TABLE VII

NET GAIN FOR DIFFERENT MAXIMUM FREE DISTANCE CONVOLUTIONAL CODE WITH CODE RATE EQUAL TO 1/2, 1/4, AND 1/8

													Net Gain								
				Y_1						Y_2			Γ_1			Γ_2			Γ_3		
	PAPR Value ($\text{CCDF} = 10^{-4}$)			ΔPAPR ($\text{CCDF} = 10^{-4}$)			SNR Value ($\text{BER} = 10^{-3}$)			SNR Variation ($\text{BER} = 10^{-3}$)			$\alpha_1 = 0.5$ $\alpha_2 = 0.5$			$\alpha_1 = 0.75$ $\alpha_2 = 0.25$			$\alpha_1 = 0.25$ $\alpha_2 = 0.75$		
V \ R	1/2	1/4	1/8	1/2	1/4	1/8	1/2	1/4	1/8	1/2	1/4	1/8	1/2	1/4	1/8	1/2	1/4	1/8	1/2	1/4	1/8
OFDM	11.52			-	-	-	10.1			-	-	-	-	-	-	-	-	-	-	-	-
3	11.58	17.70	20.14	-0.06	-6.18	-8.62	7.98	5.88	3.52	2.12	4.22	6.58	1.03	-0.98	-1.02	0.48	-3.58	-4.32	1.58	1.62	2.78
4	11.62	11.53	18.34	-0.1	-0.01	-6.82	7.95	5.21	3.18	2.15	4.89	6.92	1.03	2.44	0.05	0.46	1.22	-3.89	1.59	3.67	3.49
5	11.60	12.86	16.36	-0.08	-1.34	-4.84	7.95	5.25	2.81	2.15	4.85	7.29	1.04	1.76	1.23	0.48	0.21	-1.81	1.59	3.30	4.26
6	11.77	11.55	12.58	-0.25	-0.03	-1.06	7.49	4.83	2.35	2.61	5.27	7.75	1.18	2.62	3.35	0.47	1.30	1.14	1.90	3.95	5.55
7	11.58	17.65	15.86	-0.06	-6.13	-4.34	7.29	5.05	2.58	2.81	5.05	7.52	1.38	-0.54	1.59	0.66	-3.34	-1.38	2.09	2.26	4.56
8	11.63	11.65	15.32	-0.11	-0.13	-3.80	6.96	4.56	2.45	3.14	5.54	7.65	1.52	2.71	1.93	0.70	1.29	-0.94	2.33	4.12	4.79

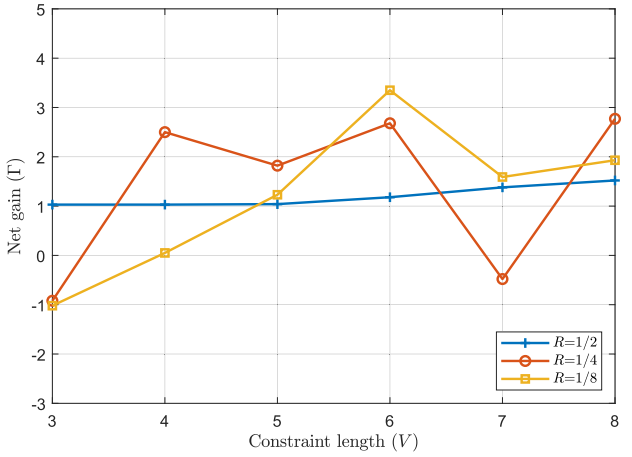

(a)

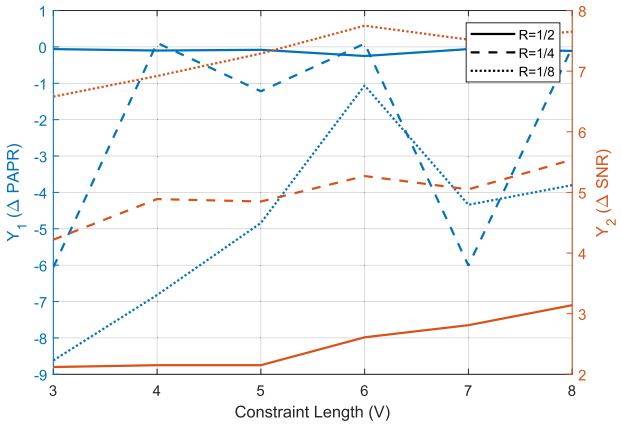

(b)

Fig. 12. (a) Net gain with $\alpha_1 = \alpha_2 = 0.5$ for different maximum free distance convolutional codes with code rate 1/2, 1/4, and 1/8, (b) Y_1 versus Y_2 for different constraint length (V) with code rate 1/2, 1/4, and 1/8.

Also, in Fig 12b, it can also seen that the variation of the SNR is in conformity with the literature results for convolutional codes, and we see that the reduction of the BER is impacted by choice of the code rate (lower code rate, greater reduction), and the constraint length. It should be remembered at this point that all the codes analyzed are the maximum free distance codes and that the distance free increases when there is an increment in the constraint length.

A. Decoder Complexity

A parameter that is an important measure to evaluate coding scheme in practice is the decoding complexity. Next we analyze the computational complexity taking as an example the convolutional codes.

If we consider a Viterbi decoder for a binary convolutional code with k input bits and constraint length V, there are $2^{k(V-1)}$ states. Therefore, there are $2^{k(V-1)}$ surviving paths at each state and $2^{k(V-1)}$ metrics [12]. The calculation of a metric is required for each path that converges at a common node, so 2^k metrics for each node is calculated. In the VA, of the 2^k paths that merge at each node, only one survives. So, in conclusion the number of calculations at each stage increases exponentially with k and V [12]. Due to this exponential growth of complexity, the VA is used mainly with short constraint lengths ($V \leq 10$).

On the other hand, the computational complexity measurement of convolutional codes for software implementations on the Viterbi algorithm operating with hard decision decoder can be defined in terms of arithmetic operation namely summations, bit comparisons and integer comparisons. McEliece and Lin [30] defined decoding complexity measure of a trellis module (repeated copies of the trellis [30]) as the total number of edge symbols in the module normalized by the number of information bits [31] called complexity of the module M that represents the additive complexity of the trellis module M. On the other hand, Benchimol *et al.* [31] raised the need to consider the computational complexity in the number of comparisons made by defining the total number of comparisons in M as the merge complexity that is equal to the total number of edges reaching it minus one [31], at a specific state of M.

We see that complexity has a considerable impact when choosing an optimal convolutional code, so, an algorithm to calculate the optimal code can be included in the calculation as described above, by considering one more parameter in the aggregate fitness value in (7), the relative increase in system complexity [15], i.e.,

$$Y_3 = -10 \log_{10} \left(\frac{\text{Complexity}_{\text{after}}}{\text{Complexity}_{\text{before}}} \right). \tag{23}$$

so the expression in (7) can be rewritten as:

$$\Gamma = \sum_{u=1}^{3} \alpha_u \cdot Y_u, \tag{24}$$

where

$$\sum_{u=1}^{3} \alpha_u = 1, \tag{25}$$

As with the computational complexity, other parameters can be added and taken into account for the selection of an optimal code in relation to the particular needs of a system and the same procedure is feasible to establish the optimal code.

VI. Conclusion

Orthogonal frequency division multiplexing (OFDM) is an attractive modulation technique for transmitting signals over wireless channels. This modulation has a lot of applications in current communications systems, and its performance can be improved by using forward error correction (FEC) codes. However, one of the main disadvantages with the OFDM system is the high peaks present in the envelope of its signal, which affects the performance of the system mainly at the level of nonlinear components.

In this work, we studied the effect of using FEC on the value of the CCDF of PAPR when a COFDM system is implemented. First, we introduced the OFDM model and discussed the exact evaluation of the CCDF of PAPR in the OFDM system. Next, we introduced the formulation of autocorrelation for uncoded and coded OFDM systems, and presented an upper bound on the peak factor of uncoded OFDM signals. Additionally, we explained a strategy for evaluating the autocorrelation for coded OFDM signals based on the Markov Chain Model, and we related the autocorrelation with the value of the CCDF of PAPR in the case of linear block codes and convolutional codes. The optimal maximum free distance convolutional codes with given constraint lengths were selected based on the value of the net gain for code rates 1/2, 1/4 and 1/8, and we concluded that the codes with $R = 1/2$, $V = 8$; $R = 1/4$, $V = 8$; and $R = 1/8$, $V = 6$ are the best option (for $\alpha_1 = \alpha_2 = 0.5$).

Finally, we concluded that based on the autocorrelation we could show some characteristics that may affect the value of the CCDF of PAPR. First, in the linear block code, the number of possible code words and the structure of the code word are important parameters. On the other hand, with convolutional codes, the important parameters are the code rate, the constraint length, and the structure of the code.

In convolutional codes, the PAPR can be increased when low code rate and relative low constraint length is used. Due to low code rate there are more options to have states that generate long chains of repetition at the output. In addition, significant structure in the convolutional encoder can increase the peak in the COFDM signal because the repetition in the output increases when there is an increment in the significant structure.

The results in the work, will contribute to correctly choosing the codes to be used in conjunction with an OFDM system in order to not increase the PAPR.

References

[1] T. Hwang, C. Yang, G. Wu, S. Li, and G. Y. Li, "OFDM and its wireless applications: A survey," *IEEE Trans. Veh. Technol.*, vol. 58, no. 4, pp. 1673–1694, May 2009. doi: 10.1109/TVT.2008.2004555.

[2] S. H. Han and J. H. Lee, "An overview of peak-to-average power ratio reduction techniques for multicarrier transmission," *IEEE Wireless Commun.*, vol. 12, no. 2, pp. 56–65, Apr. 2005. doi: 10.1109/MWC.2005.1421929.

[3] Y. Rahmatallah and S. Mohan, "Peak-to-average power ratio reduction in OFDM systems: A survey and taxonomy," *IEEE Commun. Surveys Tuts.*, vol. 15, no. 4, pp. 1567–1592, 4th Quart., 2013. doi: 10.1109/SURV.2013.021313.00164.

[4] F. Sandoval, G. Poitau, and F. Gagnon, "Hybrid peak-to-average power ratio reduction techniques: Review and performance comparison," *IEEE Access*, vol. 5, pp. 27145–27161, 2017. doi: 10.1109/ACCESS.2017.2775859.

[5] T. A. Wilkinson and A. E. Jones, "Minimisation of the peak to mean envelope power ratio of multicarrier transmission schemes by block coding," in *Proc. 21st IEEE 45th Veh. Technol. Conf. Countdown Wireless*, vol. 2, Jul. 1995, pp. 825–829. doi: 10.1109/VETEC.1995.504983.

[6] J. Tao, Z. Guangxi, and Z. Jianbin, "Block coding scheme for reducing PAPR in OFDM systems with large number of subcarriers," *J. Electron.*, vol. 21, no. 6, pp. 482–489, 2004.

[7] S. Budisin, "Golay complementary sequences are superior to PN sequences," in *Proc. IEEE Int. Conf. Syst. Eng.*, Sep. 1992, pp. 101–104. doi: 10.1109/ICSYSE.1992.236932.

[8] T. Jiang and G. Zhu, "Complement block coding for reduction in peak-to-average power ratio of OFDM signals," *IEEE Commun. Mag.*, vol. 43, no. 9, pp. S17–S22, Sep. 2005.

[9] T. Jiang and G. Zhu, "OFDM peak-to-average power ratio, reduction by complement block coding scheme and its modified version," in *Proc. IEEE 60th Veh. Technol. Conf.*, vol. 1, Sep. 2004, pp. 448–451. doi: 10.1109/VETECF.2004.1400043.

[10] A. O. Oguntade, "Range estimation for tactical radio waveforms using link budget analysis," Ph.D. dissertation, Univ. Toledo, Toledo, OH, USA, 2010.

[11] Y. Jiang, *A Practical Guide to Error-Control Coding Using MATLAB*. Norwood, MA, USA: Artech House, 2010, ch. 1, pp. 1–17.

[12] J. G. Proakis and M. Salehi, *Digital Communications*, 5th ed. New York, NY, USA: McGraw-Hill, 2008, chs. 7–8, pp. 400–589.

[13] B. Sklar, *Digital Communications: Fundamentals and Applications*, 2nd ed. Upper Saddle River, NJ, USA: Prentice-Hall, 2001, ch. 7, pp. 381–429.

[14] A. Goldsmith, *Wireless Communications*. Cambridge, MA, USA: Cambridge Univ. Press, 2004.

[15] R. Rajbanshi, "OFDM-based cognitive radio for DSA networks," Ph.D. dissertation, Inf. Telecommun. Technol. Center, Univ. Kansas, Lawrence, KS, USA, 2007.

[16] T. Jiang and Y. Wu, "An overview: Peak-to-average power ratio reduction techniques for OFDM signals," *IEEE Trans. Broadcast.*, vol. 54, no. 2, pp. 257–268, Jun. 2008. doi: 10.1109/TBC.2008.915770.

[17] T. Jiang, M. Guizani, H.-H. Chen, W. Xiang, and Y. Wu, "Derivation of PAPR distribution for OFDM wireless systems based on extreme value theory," *IEEE Trans. Wireless Commun.*, vol. 7, no. 4, pp. 1298–1305, Apr. 2008.

[18] S. G. Wilson, *Digital Modulation and Coding*. Upper Saddle River, NJ, USA: Prentice-Hall, 1995, ch. 5, p. 527.

[19] J. Mannerkoski and V. Koivunen, "Autocorrelation properties of channel encoded sequences-applicability to blind equalization," *IEEE Trans. Signal Process.*, vol. 48, no. 12, pp. 3501–3507, Dec. 2000. doi: 10.1109/78.887043.

[20] C. Tellambura, "Upper bound on peak factor of N-multiple carriers," *Electron. Lett.*, vol. 33, no. 19, pp. 1608–1609, Sep. 1997. doi: 10.1049/el:19971069.

[21] N. Y. Ermolova and P. Vainikainen, "On the relationship between peak factor of a multicarrier signal and aperiodic autocorrelation of the generating sequence," *IEEE Commun. Lett.*, vol. 7, no. 3, pp. 107–108, Mar. 2003. doi: 10.1109/LCOMM.2003.809996.

[22] G. Bilardi, R. Padovani, and G. Pierobon, "Spectral analysis of functions of Markov chains with applications," *IEEE Trans. Commun.*, vol. 31, no. 7, pp. 853–861, Jul. 1983. doi: 10.1109/TCOM.1983.1095910.

[23] N. Ngajikin, N. Fisal, and S. K. Yusof, "PAPR reduction in WLAN-OFDM system using code repetition technique," in *Proc. Student Conf. Res. Develop. (SCORED)*, Aug. 2003, pp. 85–89. doi: 10.1109/SCORED.2003.1459669.

[24] B. Moision, "A truncation depth rule of thumb for convolutional codes," in *Proc. Inf. Theory Appl. Workshop*, Jan./Feb. 2008, pp. 555–557. doi: 10.1109/ITA.2008.4601052.

[25] E. Frontana and I. Fair, "Avoiding PAPR degradation in convolutional coded OFDM signals," in *Proc. IEEE Pacific Rim Conf. Commun., Comput. Signal Process.*, Aug. 2007, pp. 312–315. doi: 10.1109/PACRIM.2007.4313237.
[26] S. Lin and D. J. Costello, *Error Control Coding: Fundamentals and Applications*, 2nd ed. Upper Saddle River, NJ, USA: Prentice-Hall, 2004, ch. 11, pp. 453–513.
[27] A. Richardson, *WCDMA Design Handbook*. Cambridge, U.K.: Cambridge Univ. Press, 2005, ch. 1, p. 7.
[28] M. Jeruchim, "Techniques for estimating the bit error rate in the simulation of digital communication systems," *IEEE J. Sel. Areas Commun.*, vol. 2, no. 1, pp. 153–170, Jan. 1984.
[29] S. H. Müller and J. B. Huber, "A comparison of peak power reduction schemes for OFDM," in *Proc. IEEE Global Telecommun. Conf. Conf. (GLOBECOM)*, vol. 1, Nov. 1997, pp. 1–5.
[30] R. J. McEliece and W. Lin, "The trellis complexity of convolutional codes," *IEEE Trans. Inf. Theory*, vol. 42, no. 6, pp. 1855–1864, Nov. 1996.
[31] I. B. Benchimol, C. Pimentel, R. D. Souza, and B. F. Uchôa-Filho, "A new computational decoding complexity measure of convolutional codes," *EURASIP J. Adv. Signal Process.*, vol. 2014, no. 1, p. 173, Dec. 2014. doi: 10.1186/1687-6180-2014-173.

Francisco Sandoval received the B.S. degree in electronic and telecommunications engineering from the Universidad Técnica Particular de Loja (UTPL) in 2008 and the M.S. degree in electrical engineering from the Pontifícia Universidade Católica do Rio de Janeiro (PUC-RIO) in 2013. He is currently pursuing the Ph.D. degree in electrical engineering with the École de Technologie Supérieure, University of Quebec, Canada. Since 2008, he has been an Assistant Professor with the Computer Science and Electronic Department (DCCE), UTPL. His research interests include wireless communications, communication theory, signal processing, and RF propagation.

Gwenael Poitau received the bachelor's and master's degrees in physics from Telecom Saint-Etienne, France, and the Ph.D. degree in electrical engineering from the Institut National des Sciences Appliquées de Lyon, France. He was with Wavesat, Montreal, where he was involved in developing signal processing algorithms and application-specified integrated circuit (ASIC) architectures for 4G chipsets. He has over 15 years of experience in developing wireless communication systems for the telecom and defense markets. He was then promoted as a Technical Lead for LTE development. He continued to work on LTE with Interdigital, where he generated intellectual property on device-to-device communications and participated to LTE Rel. 12 standardization. In 2010, he joined Ultra Electronics TCS as a Wireless Architect for the new ORION radio product line, where he was promoted as a Chief Technology Officer (CTO) in 2013. In addition to the CTO role, he was the Head of engineering in 2016. He holds nine invented patents in wireless communications. He has authored multiple IEEE publications.

François Gagnon received the B.E. and Ph.D. degrees in electrical engineering from the École Polytechnique de Montréal.

He was a Founder and the First Director of the Communications and Microelectronic Integration Laboratory (LACIME). From 1999 to 2001, he was the Director of the Department of Electrical Engineering, École de Technologie Supérieure (ÉTS), where he has been a Professor since 1991. Since 2001, he has been an Industrial Research Chair. He has been involved in the creation of the new generation of high-capacity line-of-sight military radios offered by the Ultra Electronics Tactical Communication Systems. Ultra-Electronics TCS and ÉTS have obtained the NSERC Synergy prize for this collaboration. He serves on the boards of funding agencies and companies. He specializes in wireless communications, modulation, coding, microelectronics, signal processing, equalization, software-defined radio, mobile communication, and fading channels. He is actively involved in the SmartLand project of UTPL, Ecuador, the STARACOM strategic research network, and the Réseau Québec Maritime. He is the Richard J. Marceau Industrial Research Chair for Wireless Internet in Developing Countries. He is the NSERC-Ultra Electronics Chair in Wireless Emergency and Tactical Communication, the most prestigious industrial chair program in Canada.